II

Other Topics

Numerical Relativistic Hydrodynamics

José Mª. Ibáñez

Departament de Física Teòrica, Universitat de València,
46100-Burjassot, València, Spain

Abstract: Some *high-resolution shock-capturing methods* have been designed recently to solve nonlinear hyperbolic systems of conservation laws. We have extended them to the relativistic hydrodynamic system of equations *via a local characteristic approach* . We are presenting tests of our procedure in the ultrarelativistic case. We have studied the gravitational collapse of spherically symmetric configurations. Finally, preliminary results in multidimensional applications are displayed.

1 Introduction

In the present lecture I am going to report recent preliminary results in a research project developing a fully relativistic and multidimensional hydrodynamical code. This work is currently being carried out in collaboration with José A. Font, A. Marquina, José Mª. Martí, Juan A. Miralles and José V. Romero, at the University of València.

The term *relativistic hydrodynamics* refers to that part of Physics devoted to the study of the dynamics of both those flows in which the bulk Lorentz factor $W \equiv (1 - v^2)^{-1/2}$ exceeds one in more than a few percent (v is the flow velocity in units of the speed of light) or those where the effects of the background gravitational field -or that generated by the matter itself- are so important that a description in terms of the Einstein theory of gravity must be taken into account.

Relativistic hydrodynamics plays a major role in the realm of Astrophysics. High-velocity outflows can be found in galactic jets (see, for example [2]), in the stellar collapse of iron cores into massive stars which precedes the Supernovae II explosions [9], or in the material accreting onto a compact object [59]. In galactic jets the fluid material reaches the ultrarelativistic regime (i.e., $W \geq 2$). The existence of strong gravitational fields in some of the above astrophysical scenarios complicates the problem and a fully general-relativistic description is necessary.

Our main aim is to correctly model the formation and propagation of strong shocks. Strong relativistic shocks are a very important feature in several problems arising not only in Astrophysics (see above) but also in Cosmology [46] and Plasma Physics [1].

A multidimensional description is necessary in order to understand the complex structures of these shocks when interacting with matter of the interstellar or intergalactic medium or even more interesting when dynamical instabilities of different kinds are developed (Rayleigh-Taylor, Kelvin-Helmholtz,...) at the interfaces between two fluids. Finally, a multidimensional analysis will be necessary if we are interested in describing the release -even in a quasi-Newtonian description - of gravitational radiation coming from the gravitational collapse of cores in evolved massive stars or during the collision of two compact objects.

From the numerical point of view the correct modelling of shocks has attracted the attention of many researchers in Astrophysics and in Computational Fluid Dynamics. A numerical scheme in conservation form allows for *shock-capturing*, i.e., it guarantees the correct jump conditions across discontinuities. Traditionally, shock-capturing methods introduced *artificial viscosity* terms in the scheme in order to damp the oscillations and instabilities associated with the numerical computation of discontinuities. Historically, researchers working in relativistic -both special and general- hydrodynamics (see references [56], [61]; the *Kyoto group* : [50], [49], [51]; *Wilson's school* : [10], [16], [32]), following Wilson's pioneering work ([68], [69]), have used a combination of artificial viscosity and upwind techniques in order to get numerical solutions of the relativistic hydrodynamic equations.

Wilson wrote the system as a set of advection equations. In order to do this he has to treat terms containing derivatives (in space or time) of the pressure as source terms. This procedure breaks -physically and numerically- an important property of the relativistic hydrodynamic system of equations: its *conservative* character (see below).

In recent years a number of new shock-capturing finite difference approximations have been constructed and found to be very useful in shock calculations (see, e.g., [71] and references cited therein). In addition to conservation form, these schemes are usually constructed to have the following properties:

a) Stable and sharp discrete shock profiles.

b) High accuracy in smooth regions of the flow

Schemes with these characteristics are usually known as *high-resolution schemes*. They avoid the use of artificial viscosity terms when treating discontinuities and, after extensive experimentation, they appear to be a solid alternative to classical methods with artificial viscosity. As a sample, the Piecewise Parabolic Method described in [11] has become quite popular among people interested in Newtonian astrophysical simulations.

We have recently proposed an extension of these *modern high-resolution shock-capturing methods* specifically designed to solve *nonlinear hyperbolic systems of conservation laws*. This has been applied to the relativistic hydrodynamic system of equations by Martí *et al.* in [44], which, as it is well-known, have the

important property of being the expression of *local conservation laws.* This is a crucial point in our approach.

To end this section let me set out some alternative techniques which are currently being developed in order to solve the equations of relativistic hydrodynamics numerically: *Spectral methods* and *Smooth particle hydrodynamics.*

Spectral methods:

The mathematical development of spectral methods can be found in Gottlieb and Orszag [25]. Basically, they are an extension of Fourier Analysis. Each unknown function is expanded in some characteristic polynomials (Legendre, Chebychev...) according to the boundary conditions of the problem. The main advantage of the spectral methods is their accuracy: the global error on the solution decreases exponentially with the number of degrees of freedom. The handling of shock waves with spectral methods, which is one of the most severe problems concerning these techniques - due to the Gibbs phenomenon- , is currently being studied by Bonazzola and Marck (BM) in the Relativistic Astrophysics Group at Meudon (see [4], [5], [6] and [7]). By combining moving grids and shock tracking techniques BM have obtained promising results for the 1D case in [6]. BM have developed a Newtonian pseudo-spectral 3D hydro-code and studied the gravitational collapse - infall epoch- of a rotating stellar core embedded in an external tidal potential. Preliminary results corresponding to the epoch after bounce are reported by Bonazzola and Marck in [7].

Smooth particle hydrodynamics (SPH):

Derived by Gingold and Monaghan (see, e.g., [22] and [47]) and by Lucy in [38]. Interested readers can address to the recent review by Monaghan in [48].

The classic SPH approximates the density of a Newtonian fluid with the expression

$$\rho(\mathbf{x},t) \approx \sum_a m_a \mathcal{W}(\mid \mathbf{x}-\mathbf{x}_a \mid, h_a) \tag{1}$$

where m_a is the mass of a fluid "particle" a, $\mathbf{x}_a$ is its position, the function $\mathcal{W}$ is the so-called kernel, a function strongly peaked around $\mid \mathbf{x}-\mathbf{x}_a \mid = 0$ which smooths the particle over some typical "smoothing length" h_a. The properties of the kernel $\mathcal{W}$ and its different expressions can be found in the above references. The SPH formulation of the hydrodynamic equations involves the smoothed estimates of physical quantities. The smoothed estimate of any physical quantity $A(\mathbf{x})$ is:

$$< A(\mathbf{x}) > \approx \sum_a m_a \frac{A(\mathbf{x}_a)}{\rho(\mathbf{x}_a)} \mathcal{W}(\mid \mathbf{x}-\mathbf{x}_a \mid, h_a) \tag{2}$$

The main advantage of the method -as it has been emphasized by Steinmetz and Müller in [62]- is that it does not require a computational grid, making it suitable for multidimensional applications. In reference [62] a critical discussion of the capabilities and limits of SPH has been presented via the computation of a set of problems: one-dimensional standard shock tube tests, three-dimensional simulation of the adiabatic collapse of an initially isothermal gas sphere, the encounter of a star (polytrope) and a massive black hole. Some of the conclusions of the work of Steinmetz and Müller in [62] are: i) SPH is able to get accurate results

for problems involving strong shocks. ii) To obtain reliable three-dimensional results SPH requires large particle numbers of up to several tens of thousands. iii) SPH and finite difference methods should be looked upon as complementary methods.

Some preliminary attempts in the extension of SPH to find numerical solutions of relativistic hydrodynamics have been carried out by Mann in [39].

In the next section (§2) I will set out some basic notions of the theory of hyperbolic systems. Section §3 reviews some historical finite-difference schemes pointing out the fundamental differences among them. Section §4 is devoted to Godunov-type methods with which we are mainly concerned. Due to its importance the particular Riemann solver derived by Roe is presented in section §5. The theoretical ingredients recorded so far are applied to the relativistic hydrodynamic system of equations in section §6. The two particular algorithms used in our calculations are explained in section §7. The two final sections §8 and §9 focus on our one-dimensional and multi-dimensional calculations. The last section §10 summarizes our results.

2 Some definitions and reminders

Let me first give some definitions and several fundamental ideas concerning the solutions of the initial-value problem (IVP) for hyperbolic systems of conservation laws.

A one dimensional *hyperbolic system of conservation laws* is:

$$\frac{\partial \mathbf{u}}{\partial \mathrm{t}} + \frac{\partial \mathbf{f}(\mathbf{u})}{\partial \mathrm{x}} = 0 \tag{3}$$

where $\mathbf{u}$ is the N-dimensional vector of unknowns and $\mathbf{f}(\mathbf{u})$ are N-vector-valued functions called *fluxes* . The above system (3) is said to be *strictly hyperbolic* if the Jacobian matrix

$$\mathbf{A} = \frac{\partial \mathbf{f}(\mathbf{u})}{\partial \mathbf{u}} \tag{4}$$

has real and distinct eigenvalues $\{\lambda_\alpha(\mathbf{u})\}_{\alpha=1,..\mathrm{N}}$ and the set of eigenvectors is complete in $\mathcal{R}^N$. If some of the eigenvalues are equal the system is a non-strictly hyperbolic one. We will assume that the eigenvalues are arranged in increasing order.

The equation

$$dx/dt = \lambda_\alpha(\mathbf{u}) \tag{5}$$

defines the α^{th} *characteristic field* .

Lax [36] has shown that the above IVP has at most one C^1 solution (*classical solution*) in the small. In the large, discontinuous solutions (*weak solutions*) are admitted. A weak solution is one that satisfy (3) in the sense of distribution theory, i.e.,

$$\int_0^\infty \int_{-\infty}^\infty \left(\frac{\partial \omega}{\partial t}\mathbf{u} + \frac{\partial \omega}{\partial \mathrm{x}}\mathbf{f}(\mathbf{u}) \right) dxdt + \int_{-\infty}^\infty \omega(x,0)\mathbf{u}_0(x)dx = 0 \tag{6}$$

for all C^∞ test functions $\omega(x,t)$ that vanish for $\mid x \mid + t$ large. This is equivalent to requiring that the relation obtained by integrating (3) over the rectangle $(a,b) \times (t_1,t_2)$ should hold:

$$\int_a^b \mathbf{u}(\mathrm{x},\mathrm{t}_2)\mathrm{dx} - \int_{\mathrm{a}}^{\mathrm{b}} \mathbf{u}(\mathrm{x},\mathrm{t}_1)\mathrm{dx} + \int_{\mathrm{t}_1}^{\mathrm{t}_2} \mathbf{f}(\mathbf{u}(\mathrm{b},\mathrm{t}))\mathrm{dt} - \int_{\mathrm{t}_1}^{\mathrm{t}_2} \mathbf{f}(\mathbf{u}(\mathrm{a},\mathrm{t}))\mathrm{dt} = 0 \quad (7)$$

A piecewise-smooth weak solution of (3) satisfies (3) pointwise in each smooth region; across each curve of discontinuity the *Rankine-Hugoniot relation* (R-H)

$$\mathbf{f}(\mathbf{u}_R) - \mathbf{f}(\mathbf{u}_L) = s(\mathbf{u}_R - \mathbf{u}_L) \quad (8)$$

holds, where s is the propagation speed of discontinuity, and $\mathbf{u}_R$ and $\mathbf{u}_L$ are, respectively, the states on the right and on the left of the discontinuity.

The class of all weak solutions is too wide in the sense that there is no uniqueness for the IVP, and an additional principle is needed for determining the physically relevant solution. Usually this principle -sometimes called *viscosity principle*- identifies the physically relevant solutions, defined as those that are the limit as $\epsilon \to 0$ of solutions $\mathbf{u}(\epsilon)$ of the viscous equations.

$$\frac{\partial \mathbf{u}}{\partial t} + \frac{\partial \mathbf{f}(\mathbf{u})}{\partial x} = \epsilon \frac{\partial^2 \mathbf{u}}{\partial x^2} \quad , \quad \epsilon > 0 \quad (9)$$

For the scalar case, Oleinik in [54] has shown that discontinuities of such admissible solutions can be characterized by the following condition:

$$\frac{f(u) - f(u_L)}{u - u_L} \geq s \geq \frac{f(u) - f(u_R)}{u - u_R} \quad (10)$$

for all values of u between u_L and u_R (*entropy condition*). A discontinuity is called a *shock* if the above inequalities are strict. A discontinuity is called a *contact* discontinuity if equalities hold identically. If f is convex the above characterization is equivalent to

$$u_L \geq u_R \quad (11)$$

or

$$f'(u_L) \geq s \geq f'(u_R) \quad (12)$$

where primes stand for derivative with respect to the argument. This last relation has a geometrical interpretation: the characteristic curves at each side must converge to the discontinuity curve.

For systems of conservation laws, Lax has given the corresponding characterization of the admissible solutions to (3). For a given α, it is

$$\lambda_\alpha(\mathbf{u}_L) \geq s \geq \lambda_\alpha(\mathbf{u}_R) \quad (13)$$

$$\lambda_{\alpha-1}(\mathbf{u}_L) < s < \lambda_{\alpha+1}(\mathbf{u}_R) \quad (14)$$

These relations guarantee that α fields of characteristics converge to the discontinuity curve from the right and $N - \alpha + 1$ from the left. The information

carried by these $N+1$ characteristic curves and the $N-1$ relations that we can derive from the R-H conditions, when s is eliminated, allows to know the $2N$ values of **u** at each side of the discontinuity.

In the following we will focus on numerical approximations to weak solutions of (3), $v(x,t)$, that are obtained by explicit schemes in *conservation form* :

$$v_j^{n+1} = v_j^n - \lambda(\widehat{f}_{j+1/2} - \widehat{f}_{j-1/2}) \tag{15}$$

where $\lambda = \frac{\Delta t}{\Delta x}$, $v_j^n = v(n\Delta t, j\Delta x)$, and $\widehat{f}_{j+1/2} = \widehat{f}(v_j^n, v_{j+1}^n)$ is a *numerical flux* which must verify the consistency relation $\widehat{f}(u,u) = f(u)$.

Lax and Wendroff proved in [37] that if a finite-difference scheme in conservation form converges to some function $\mathbf{u}(x,t)$ as the grid is refined, then this function will in fact be a weak solution of the conservation law. Harten *et al.* showed in [28] that, in the scalar case, *monotonic schemes* in conservation form always converge to the physically relevant solution. Finally, a practical advantage of writing a finite-difference scheme in conservation form is that the quantities which ought to be conserved, according to the differential equation, are exactly conserved in the difference form.

3 Some historical finite-difference schemes

Let me pay attention to three classical finite-difference schemes proposed by several authors in the fifties for solving the scalar hyperbolic equation

$$\frac{\partial u}{\partial t} + \frac{\partial f(u)}{\partial x} = 0 \tag{16}$$

$$a = df/du \tag{17}$$

each of them having some particular feature that is worthwhile to notice.

UPWIND (Courant *et al.* [13]):

It was the first in pointing out the role of characteristics in the numerical solution. Let us consider a be a constant, the upwind algorithm reads:

$$v_j^{n+1} = v_j^n - \lambda a(v_{j+1}^n - v_j^n) \tag{18}$$

for $a < 0$, or

$$v_j^{n+1} = v_j^n - \lambda a(v_j^n - v_{j-1}^n) \tag{19}$$

for $a > 0$.

By introducing the notation

$$a^- \equiv min(a,0) = \frac{1}{2}(a - \mid a \mid) \tag{20}$$

$$a^+ \equiv max(a,0) = \frac{1}{2}(a + \mid a \mid) \tag{21}$$

we can rewrite the upwind algorithm in several forms

$$v_j^{n+1} = v_j^n - \lambda \left[(a^+(v_j^n - v_{j-1}^n) + a^-(v_{j+1}^n - v_j^n) \right] \tag{22}$$

or,

$$v_j^{n+1} = \lambda a^+ v_{j-1}^n + (1 - \lambda \mid a \mid) v_j^n - \lambda a^- v_{j+1}^n \tag{23}$$

or,

$$v_j^{n+1} = v_j^n - \frac{\lambda}{2} a (v_{j+1}^n - v_{j-1}^n) + \frac{\lambda}{2} \mid a \mid (v_{j+1}^n - 2v_j^n + v_{j-1}^n) \tag{24}$$

The last equation displays the conservative form of the scheme by defining the numerical flux:

$$\widehat{f}_{j+1/2}^U = \frac{1}{2} \left[a(v_{j+1}^n + v_j^n) - \mid a \mid (v_{j+1}^n - v_j^n) \right] \tag{25}$$

If a is not a constant, then, a generalization of the upwind scheme is

$$\widehat{f}_{j+1/2}^U = \frac{1}{2} \left[f_{j+1} + f_j - \mid a_{j+1/2} \mid (v_{j+1}^n - v_j^n) \right] \tag{26}$$

Equation (23) shows the monotone character of the scheme provided that the condition $\sigma \equiv \lambda \mid a \mid \leq 1$ is satisfied. This is the Courant-Friedrich-Lewy condition (CFL) which expresses the fact that the dependence domain of the solution of the finite difference equation must include the dependence domain of the solution of the partial differential equation at all grid points.

GODUNOV [24]:

As the upwind scheme, the Godunov method -in its original formulation- is first order accurate. We will pay particular attention to this scheme in section §4, which, in a generic conservative form, can be written as

$$v_j^{n+1} = v_j^n - \lambda (\widehat{f}_{j+1/2}^G - \widehat{f}_{j-1/2}^G) \tag{27}$$

TWO-STEP LAX-WENDROFF [37]:

In the nonlinear case, the two-step Lax-Wendroff (LW) scheme can be written in a conservative form

$$v_j^{n+1} = v_j^n - \lambda (\widehat{f}_{j+1/2}^{LW} - \widehat{f}_{j-1/2}^{LW}) \tag{28}$$

where the LW-numerical flux is defined by

$$\widehat{f}_{j+1/2}^{LW} = f(v_{j+1/2}^{n+1/2}) \tag{29}$$

$$v_{j+1/2}^{n+1/2} = \frac{1}{2}(v_{j+1}^n + v_j^n) - \frac{\lambda}{2} \left(f(v_{j+1}^n) - f(v_j^n) \right) \tag{30}$$

The LW scheme is second-order accurate, both in space and time, provided that the CFL condition be satisfied.

Let us comment on some peculiarities which can arise, in a numerical application, if we, naively, choose the LW scheme guided only by its high accuracy. In [28] an example is given of a solution to the above scalar hyperbolic conservation law with $f(u) = u - 3\sqrt{3}\, u^2(u-1)^2$ and initial condition $u(x,0) = 1$ if $x \leq 0.5$ or $u(x,0) = 0$ if $x > 0.5$. The numerical results indicated that the

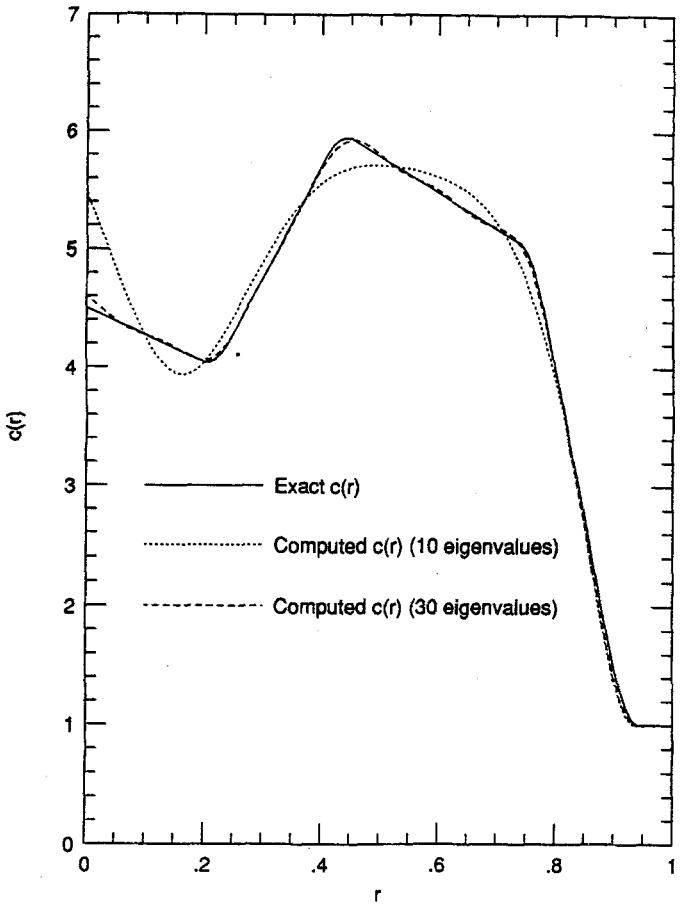

Acknowledgement The author's research was partially supported by ONR Grant N00014-91J-1166.

References

[CM] Colton, D., Monk, P.: The inverse scattering problem for time-harmonics acoustic waves in an inhomogeneous medium. Q. J. Mech. and Math. 41 (1988) 97–125.

[GL] Gel'fand, I. M., Levitan, B. M.: On the determination of a differential equation from its spectral function. Amer. Math. Soc. Trans. 1 (1951) 253–304.

[HW] Hartman, P., Wilcox, C.: On solutions of the Helmholtz equation in exterior domains. Math. Zeit. 75 (1961) 228–255.

[MP] McLaughlin, J. R., Polyakov, P.L: On the uniqueness of a spherically symmetric speed of sound from transmission eigenvalues. To appear in J. Diff. Eq.

[MPS] McLaughlin, J. R., Polyakov, P. L., Sacks, P. E.: Reconstruction of a spherically symmetric speed of sound. Submitted.

[RS] Rundell, W., Sacks, P. E.: The Reconstruction of Sturm-Liouville Operators. Inverse Problems 8 (1992) 457–482.

noticed in [20], not only is the convergence of the viscosity method for general strictly hyperbolic systems still an open question, but this approach is, in general, not well-behaved when the system is a non-strictly hyperbolic one.

4 Godunov-type methods

In 1959 Godunov described in [24] an ingenious method for one-dimensional fluid dynamic problems with shocks. Let $j-1/2$ and $j+1/2$ be the lower and the upper interfaces, respectively, of the numerical cell j. Godunov's original idea was to consider that there is a real discontinuity at the interface of the variables of our problem, and, consequently, he proposed using the exact solution of *local Riemann problems* .

A Riemann problem is an *initial value problem* for (3) with initial data:

$$\mathbf{u}(\mathrm{x},0)=\begin{cases}\mathbf{u}_{\mathrm{L}} & \text{if } x<x_{shell}\\ \mathbf{u}_{\mathrm{R}} & \text{if } x>x_{shell}\end{cases}$$

where $\mathbf{u}_{\mathrm{L,R}}$ are constant states left and right of a given discontinuity at $x=x_{shell}$.

In general, the solution of that Riemann problem depends only on the states $\mathbf{u}_{\mathrm{L}}$, $\mathbf{u}_{\mathrm{R}}$ and the ratio x/t; it will be denoted by $\mathbf{u}\left((x-x_{shell})/t;\mathbf{u}_L,\mathbf{u}_R\right)$.

The main features of the *Godunov's algorithm* are (see [43], for details)

1) It is written in *conservation form*

$$\mathbf{u}_j^{n+1}=\mathbf{u}_j^n-\frac{\Delta t}{\Delta x}(\widehat{\mathbf{f}}_{j+1/2}-\widehat{\mathbf{f}}_{j-1/2}) \tag{32}$$

where $\widehat{\mathbf{f}}$ is the *numerical flux* (see below), $\mathbf{u}_j^{n+1}$ is

$$\mathbf{u}_j^{n+1}=\frac{1}{\Delta x}\int_{I_j}\mathbf{u}_{\mathrm{n}}(\mathrm{x},\mathrm{t}_{\mathrm{n}+1})\mathrm{dx} \tag{33}$$

The above integration is carried out into the numerical cell $I_j=[(j-1/2)\Delta x,(j+1/2)\Delta x]$ and $\mathbf{u}_{\mathrm{n}}(\mathrm{x},\mathrm{t})$ can be expressed exactly in terms of the solution of local Riemann problems:

$$\mathbf{u}_n(x,t)=\begin{cases}\mathbf{u}\left(\frac{x-(j+1/2)\Delta x}{t-t_n};\mathbf{u}_j^n,\mathbf{u}_{j+1}^n\right) & \text{if } j\Delta x<x<(j+1/2)\Delta x\\ \mathbf{u}\left(\frac{x-(j-1/2)\Delta x}{t-t_n};\mathbf{u}_{j-1}^n,\mathbf{u}_j^n\right) & \text{if } (j-1/2)\Delta x<x<j\Delta x\end{cases}$$

with $t_n\le t\le t_{n+1}$

The theorem of Lax and Wendroff [37] -see at the end of section §2- assures that a weak solution can be found. Harten *et al.* in [30] showed that the exact solution $\mathbf{u}_{\mathrm{n}}(\mathrm{x},\mathrm{t})$ satisfies the entropy condition.

2) The *numerical flux*, $\widehat{\mathbf{f}}$, is defined by

$$\widehat{\mathbf{f}}_{j+1/2}=\mathbf{f}(\widehat{\mathbf{u}}_{j+1/2})$$

where

$$\widehat{\mathbf{u}}_{j+1/2} = \mathbf{u}(0; \mathbf{u}_j^n, \mathbf{u}_{j+1}^n)$$

is the exact solution of the Riemann problem at the interface $x = (j + 1/2)\Delta x$.

The exact solution of this problem for the dynamics of ideal gases can be found, for example, in reference [57] and the corresponding algorithm will be called *Godunov's Riemann solver* .

When $\mathbf{u}_n(x,t)$ is some approximation to the exact solution of the Riemann problem, then, the scheme is called a *Godunov-type* method (see, e.g., references [30], [65], [14], [21]).

The original Godunov method is only first order accurate. The renewed interest in these methods arises after the works of Van Leer ([63], [64]) which focus on the improvements of the spatial accuracy by cell-reconstruction techniques.

Given the computational cost involved in solving exactly the Riemann problem for general nonlinear hyperbolic systems of conservation laws or for materials with a general equation of state (EOS), several *approximate Riemann solvers* have been derived in recent years ([58], [12], [14] [23]).

5 Roe's Riemann solver

Given the importance of this seminal technique we are going to point out the main steps leading to the so-called *Roe's numerical flux*. The following discussion of Roe's Riemann solver is taken from [58] (see, also [43] for details).

Roe looks for approximate solutions of the above Riemann problem which are exact solutions to the approximate problem resulting when the original Jacobian matrix $\mathbf{A}$ of the system (3) is replaced by a new matrix $\widetilde{\mathbf{A}}$ such that: i) $\widetilde{\mathbf{A}}$ is a constant matrix that depends only on the initial data. ii) As $\mathbf{u}_L$ and $\mathbf{u}_R \rightarrow \mathbf{u}$ is

$$\widetilde{\mathbf{A}}(\mathbf{u}_L, \mathbf{u}_R) \rightarrow \mathbf{A}(\mathbf{u})$$

this is a *consistency relation.* iii) For any $\mathbf{u}_L$ and $\mathbf{u}_R$ is

$$\widetilde{\mathbf{A}}(\mathbf{u}_L, \mathbf{u}_R).(\mathbf{u}_L - \mathbf{u}_R) = \mathbf{f}_L - \mathbf{f}_R$$

iv) The eigenvectors of $\widetilde{\mathbf{A}}$ are *linearly independent.*

The conditions iii) and iv) are necessary and sufficient for the algorithm to recognize a shock wave.

In this way, the numerical fluxes can be written

$$\widehat{\mathbf{f}}(\mathbf{u}_\mathrm{L}, \mathbf{u}_\mathrm{R}) = \frac{1}{2}(\mathbf{f}_\mathrm{L} + \mathbf{f}_\mathrm{R} - \sum_{\alpha=1}^{N} \mid \widetilde{\lambda}_\alpha \mid \Delta\widetilde{\omega}_\alpha \widetilde{\mathbf{e}}_\alpha) \tag{34}$$

where $\widetilde{\lambda}_\alpha$ and $\widetilde{\mathbf{e}}_\alpha$ $(\alpha = 1, ..., N)$ are the eigenvalues (*characteristic speeds*) and the eigenvectors of the Jacobian $\widetilde{\mathbf{A}}$, respectively. The quantities $\Delta\widetilde{\omega}_\alpha$ are the jumps of the *local characteristic variables* across discontinuities and are obtained from:

$$\mathbf{u}_{\mathrm{R}} - \mathbf{u}_{\mathrm{L}} = \sum_{\alpha=1}^{\mathrm{N}} \Delta\tilde{\omega}_{\alpha}\tilde{\mathbf{e}}_{\alpha} \tag{35}$$

Some comments are in order:

1. Since the scheme is based on a linear decomposition of the characteristic fields, one can apply different numerical schemes for each field.
2. The scheme is non-oscillatory in the sense that no new extrema are created for the linear systems or a single nonlinear conservation law. No spurious numerical oscillations contaminate the calculations.
3. The above construction gives a difference approximation of first-order accuracy and may admit entropy violating shocks. Transonic rarefactions may generate unphysical solutions; they are prevented by adding some artificial viscosity only at the sonic points (see, for example, [29]).
4. By construction Roe's Riemann solver is exact for constant coefficient linear system of conservation laws.

Further details can be found in [58].

6 The equations of Relativistic Hydrodynamics as a system of conservation laws

The fundamental equations of motion describing a relativistic fluid flow are governed by *local conservation laws*: the local conservation of baryon number density

$$\nabla_{\mu} J^{\mu} = 0 \tag{36}$$

and the local conservation of energy-momentum

$$\nabla_{\nu} T^{\mu\nu} = 0 \tag{37}$$

where the current J^{μ} and the energy-momentum tensor $T^{\mu\nu}$ are

$$J^{\mu} = \rho u^{\mu} \tag{38}$$

$$T_{\mu\nu} = \rho h u_{\mu} u_{\nu} + p g_{\mu\nu} \tag{39}$$

($\alpha = 0, 1, 2, 3$ and latin indices run from 1 to 3). In the above equations ρ is the rest-mass density, p is the pressure, h is the specific enthalpy, $h = 1 + \epsilon + p/\rho$, ϵ is the specific internal energy, u^{μ} is the four-velocity of the fluid and $g_{\mu\nu}$ defines the space-time $\mathcal{M}$ where the fluid evolves.

We have constrained the energy-momentum tensor to be a perfect fluid, neglecting heat conduction, viscous interactions and magnetic fields. The Minkowski metric is used throughout, that is, gravitational effects of any nearby bodies and of the fluid itself have been neglected.

In Cartesian coordinates the above system of equations (36, 37) can be written in a more explicit way

$$\frac{\partial \mathbf{F}^{\alpha}(\mathbf{w})}{\partial x^{\alpha}} = 0 \tag{40}$$

where the 5-vector of unknowns is

$$\mathbf{w} = (\rho, \mathrm{v_i}, \epsilon) \tag{41}$$

and the quantities $\mathbf{F}^\alpha$ are

$$\mathbf{F}^0(\mathbf{u}) = (\rho W, \rho h W^2 v_j, \rho h W^2 - p) \tag{42}$$

$$\mathbf{F}^i(\mathbf{u}) = (\rho W v_i, \rho h W^2 v^i v_j + p\delta^i_j, \rho h W^2 v^i) \tag{43}$$

In the above expressions is $x^\alpha = (t, x, y, z)$, the three-velocity $v^i \equiv u^i/u^0$ has the components $v^i = (v^x, v^y, v^z)$ and the Lorentz factor defined by $W \equiv u^0$ satisfies the familiar relation $W = (1 - v^2)^{-1/2}$ ($v^2 = \delta_{ij} v^i v^j$). The components of $\mathbf{F}^0(\mathbf{w})$ are, respectively, the relativistic rest-mass density, the relativistic momentum density and the total energy density.

An equation of state $p = p(\rho, \epsilon)$ closes, as usual, the system. A very important quantity derived from the equation of state is the local sound velocity c_s:

$$h c_s^2 = \chi + (p/\rho^2)\kappa \tag{44}$$

with $\chi = \partial p/\partial \rho$ and $\kappa = \partial p/\partial \epsilon$.

From the computational point of view, the last equation of the system (40) is not very useful since, in the Newtonian limit ($p \simeq \rho\epsilon << \rho$, $v << 1$) and for all practical purposes, this equation is identical to the first one. In practice, the last equation has been substituted by the one which results when subtracting the first one from it.

The set of equations (40) constitutes a particular quasi-linear system of 5 first order partial differential equations for the unknown field $\mathbf{w}$, for which the (5×5)-matrices $\mathcal{A}^\alpha(\mathbf{w})$ are the Jacobian matrices associated to the 5-vector $\mathbf{F}^\alpha(\mathbf{w})$, the *flux* in the α-direction. The explicit expressions of the matrices $\mathcal{A}^\alpha$ can be found in reference [19]. System (40) can be rewritten as

$$\mathcal{A}^\alpha(\mathbf{w}) \frac{\partial \mathbf{w}}{\partial x^\alpha} = 0 \tag{45}$$

The hyperbolic character of system (45) has been exhaustively studied by Anile and collaborators (see [1] and references cited therein) for a general space-time in which the fluid evolves (*test fluid approximation*). In particular, they have derived the spectral decomposition of the above Jacobian matrices in the particular reference frame for which matter is at rest. In [19] we have generalized this analysis for an arbitrary reference frame filling, as far as we know, a gap in the scientific literature.

According to Anile [1] the above system (45) will be hyperbolic in the time-direction defined by the vector field ξ with $\xi_\alpha \xi^\alpha = -1$, if the following two conditions hold:

i) $\det(\mathcal{A}^\alpha \xi_\alpha) = 0$

ii) for any ζ such that $\zeta_\alpha \xi^\alpha = 0$, $\zeta_\alpha \zeta^\alpha = 1$, the eigenvalue problem

$$\mathcal{A}^\alpha(\zeta_\alpha - \lambda \xi_\alpha)\mathbf{r} = 0 \tag{46}$$

has only real eigenvalues λ and N linearly independent eigenvectors $\mathbf{r}$.

These conditions have a particular interest from a technical point of view. We will return to this point at the end of this section.

Equations (40) can be written as a system of *conservation laws in the sense of Lax* [36] allowing to apply specific numerical techniques for solving them numerically. With this aim let us define the vector

$$\mathbf{u} = \mathbf{F}^0(\mathbf{w}) \tag{47}$$

and let us introduce the three 5-vectors $\mathbf{f}^i$ defined by

$$\mathbf{f}^i = \mathbf{F}^i \circ (\mathbf{F}^0)^{-1} \tag{48}$$

where $\circ$ means composition of functions.

With the above definitions, system (40) reads as a system of conservation laws in the sense of Lax [36] for the new vector of unknowns $\mathbf{u}$

$$\frac{\partial \mathbf{u}}{\partial x^0} + \frac{\partial \mathbf{f}^i(\mathbf{u})}{\partial x^i} = 0 \tag{49}$$

In the above system (49) we can define (5×5)-Jacobian matrices $\mathcal{B}^i(\mathbf{u})$, the Jacobian matrices associated to the 5-vector $\mathbf{f}^i(\mathbf{u})$, the so-called *flux* in the j-direction of the system (49) as:

$$\mathcal{B}^i = \frac{\partial \mathbf{f}^i(\mathbf{u})}{\partial \mathbf{u}} \tag{50}$$

Let $\{\lambda_\alpha, \mathbf{r}_\alpha\}$ be, respectively, the eigenvalues and righteigenvectors of matrices $\mathcal{A}^i$ solution of the eigenvalue problem (46). Then the following result is easy to verify: the spectral decomposition of the Jacobian matrices $\mathcal{B}^i$ is given by the set $\{\lambda_\alpha, \mathcal{A}^0\mathbf{r}_\alpha\}$. All these quantities are known in terms of the original variables $\mathbf{w}$ (see reference [19] for more details).

The above conclusion sets up the technical ingredients for extending modern high-resolution shock-capturing methods to multidimensional relativistic hydrodynamics.

7 Two high-resolution shock-capturing algorithms: MUSCL and PHM

Let

$$\frac{\partial \mathbf{u}}{\partial \mathrm{t}} + \frac{\partial \mathbf{f}(\mathbf{u})}{\partial \mathrm{x}} = \mathbf{s}(\mathbf{u}) \tag{51}$$

a one dimensional *hyperbolic system of conservation laws* with *source terms* $\mathbf{s}(\mathbf{u})$. Strictly speaking a conservation law implies that the source term is zero. In practice, these terms may have an important influence in the calculations as a

source of numerical difficulties. Hence, I will consider, in the next, hyperbolic systems like (51).

Two modern high-resolution shock-capturing algorithms have been implemented into our relativistic hydro-code: i) Our version of MUSCL (from Monotonic Upstream Schemes for Conservation Laws [64]), which is globally second order accurate, and ii) PHM (from Piecewise Hyperbolic Method, designed by Marquina in [40]).

Let us summarize the main features of both algorithms in the next subsections.

7.1 Our MUSCL-version

The main ingredients of our MUSCL algorithm - an approximate Riemann solver and cell reconstruction techniques- were presented in [44]. Let me describe them in some detail.

1. At each time level, the data are the *cell averages* of the conserved quantities

$$\mathbf{v}_j^n = \frac{1}{\Delta x_j} \int_{x_{j-1/2}}^{x_{j+1/2}} \mathbf{u}(x, t^n) dx \tag{52}$$

2. *Reconstruction procedure* of the solution from its cell averages:
   A monotonicity preserving linear reconstruction of the original variables using the 'minmod' function as a 'slope limiter' (see reference [64]).
3. Evaluation of the *numerical fluxes* at the cell interfaces:
   The i^{th} component of the numerical flux is computed as follows

$$\widehat{f}^{(i)}_{j+\frac{1}{2}} = \frac{1}{2}\left(f^{(i)}(\mathbf{u}^L_{j+\frac{1}{2}}) + f^{(i)}(\mathbf{u}^R_{j+\frac{1}{2}}) - \sum_{\alpha=1}^{3} \mid \widetilde{\lambda}_\alpha \mid \Delta\widetilde{\omega}_\alpha \widetilde{R}^{(i)}_\alpha \right) \tag{53}$$

   where L and R stand for the left and right states at a given interface $(j+\frac{1}{2})$, $\widetilde{\lambda}_\alpha$ and $\widetilde{R}^{(i)}_\alpha$ $(\alpha = 1,2,3)$ are, respectively, the eigenvalues (i.e., the *characteristic speeds*) and the i^{th}-component of the α-righteigenvector of the Jacobian matrix

$$\mathbf{A}_{j+\frac{1}{2}} = \left(\frac{\partial \mathbf{f}(\mathbf{u})}{\partial \mathbf{u}} \right)_{\mathbf{u}=(\mathbf{u}^L_{j+\frac{1}{2}} + \mathbf{u}^R_{j+\frac{1}{2}})/2} \tag{54}$$

   and the quantities $\Delta\widetilde{\omega}_\alpha$ - the jumps in the local characteristic variables across each cell interface- are obtained from:

$$u^{(i)}_R - u^{(i)}_L = \sum_{\alpha=1}^{3} \Delta\widetilde{\omega}_\alpha \widetilde{R}^{(i)}_\alpha \tag{55}$$

   $\widetilde{\lambda}_\alpha$, $\widetilde{\mathbf{R}}^{(i)}_\alpha$ and $\Delta\widetilde{\omega}_\alpha$, as functions of $\mathbf{u}$, are evaluated at each interface and, therefore, they depend on the particular values $\mathbf{u}_L$ and $\mathbf{u}_R$.
4. *Time evolution* :
   The 'method of lines' version of the scheme is:

$$\frac{d\mathbf{u}_j(t)}{dt} = -\frac{\hat{\mathbf{f}}_{j+\frac{1}{2}} - \hat{\mathbf{f}}_{j-\frac{1}{2}}}{\Delta x} + \mathbf{s}_j \tag{56}$$

where

$$\hat{\mathbf{f}}_{j+\frac{1}{2}} = \widetilde{\mathbf{f}}(\mathbf{u}_{j-k}, \mathbf{u}_{j-k+1}, ..., \mathbf{u}_{j+k}) \tag{57}$$

is a consistent numerical flux vector, i.e., $\widetilde{\mathbf{f}}(\mathbf{u}, ..., \mathbf{u}) = \mathbf{f}(\mathbf{u})$. Once the procedure to evaluate $\hat{\mathbf{f}}_{j+\frac{1}{2}}$ is known, the system (56) can be integrated in time by using a suitable ODE (ordinary differential equation) solver.
MUSCL advances in time by a standard predictor-corrector method. This version of MUSCL is, then, globally second order accurate. In our multidimensional applications, MUSCL have used a third order Runge-Kutta method that preserves the conservation form of the scheme and does not increase the total variation of the solution at each time substep (see Shu and Osher in [60]).

7.2 PHM

The numerical results obtained in our tests (see [44]) made our updated MUSCL method reliable for the exploration of the ultrarelativistic regime. When the Lorentz factor increased we observed that our numerical scheme became less resolutive, and, consequently, we started looking for shock-capturing methods of higher resolution power.

With this aim, we approximated the solution to the equations of special-relativistic hydrodynamics in conservation form (1D planar case), by means of a third order shock-capturing method designed by Marquina [40] for 1D and 2D scalar conservation laws. We have used a *local characteristic approach* formulated by Harten *et al.* in [27] as a procedure for extending to systems Marquina's method.

Let me describe some of the technical components of PHM

1. At each time level, the data are the *point values* of the conserved quantities

$$\mathbf{v}_j^n = \mathbf{u}(x_j, t^n) \tag{58}$$

2. Evaluation of the *numerical fluxes* at the cell interfaces:
   1) Obtain the fluxes $\mathbf{g}$ of the local characteristic variables at the center of each cell as

$$\mathbf{g}_j = \mathbf{R}_j^{-1}\mathbf{f}_j \tag{59}$$

   where $\mathbf{R}_j$ is a matrix whose columns are the right eigenvectors of the Jacobian matrix

$$\mathbf{A}_j = \left(\frac{\partial \mathbf{f}(\mathbf{u})}{\partial \mathbf{u}}\right)_j \tag{60}$$

   2) With the data $\mathbf{g}_{j-1}, \mathbf{g}_j$ and $\mathbf{g}_{j+1}$, construct, componentwise, a hyperbola in $I_j = [x_{j-\frac{1}{2}}, x_{j+\frac{1}{2}}]$ as in [40].
   3) Evaluate $\widehat{\mathbf{g}}_{j+\frac{1}{2}}$, the numerical flux of the local characteristic variables at

the cell interface as in reference [40].

4) Compute $\widehat{\mathbf{f}}_{j+\frac{1}{2}}$ as follows

$$\widehat{\mathbf{f}}_{j+\frac{1}{2}} = \overset{*}{\mathbf{R}}_{j+\frac{1}{2}} \, \widehat{\mathbf{g}}_{j+\frac{1}{2}} \tag{61}$$

where each column in $\overset{*}{\mathbf{R}}_{j+\frac{1}{2}}$ is computed from hyperbolic reconstructions of the corresponding right eigenvectors of $\mathbf{A}_j$ or $\mathbf{A}_{j+1}$ according to the direction of each local characteristic wind as determined from the sign of the eigenvalues of $\mathbf{A}_j$ and $\mathbf{A}_{j+1}$.

3. *Time evolution*
PHM uses the third order Runge-Kutta method of Shu and Osher [60]. PHM is globally third order accurate.

7.3 General comments

Both algorithms are written in conservation form, thus the Rankine-Hugoniot conditions are automatically satisfied for each discontinuity, according to the Lax and Wendroff theorem cited above (section §2).

The *source terms* $\mathbf{s}_j$ can be calculated, to linear accuracy, from the values of the variables at the zone centres and at the previous time step. Nevertheless, particular caution must be taken with the source terms in the case of stiff problems. Several *time-splitting* algorithms allow to gain the accuracy required. An exact second order algorithm is the *Strang splitting* (see reference [71]) which can be written in a compact way

$$\mathbf{u}^{n+1} = \mathcal{L}_s^{\Delta t/2} \mathcal{L}_f^{\Delta t} \mathcal{L}_s^{\Delta t/2} \mathbf{u}^n \tag{62}$$

In the above equation $\mathcal{L}_f$ is the operator in finite differences which solves the homogeneous part of system (3). On the other hand $\mathcal{L}_s$ is the one that solves a system of ordinary differential equations of the form

$$\frac{\partial \mathbf{u}}{\partial \mathrm{t}} = \mathbf{s}(\mathbf{u})$$

The local characteristic approach used to extend Marquina's method to systems has proven to be extremely fruitful (see next section and reference [41]). Although both procedures require knowledge of the spectral decomposition of the Jacobian matrix, reconstructing the fluxes of the local characteristic variables (as in PHM) eliminates the "noise" around the points where the discontinuities of $\mathbf{u}(\mathrm{x}, \mathrm{t})$ interact (or are very close).

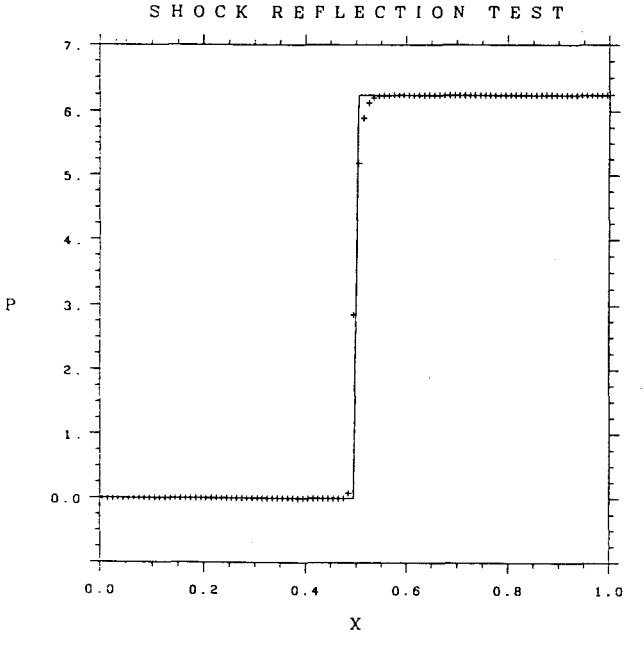

Fig. 1. Pressure in the *relativistic shock wall* test. Initial velocity is 0.9, in units of the speed of light

8 1D Relativistic Hydrodynamics: tests and applications.

In this section we will see how our hydro-code works in one-dimensional applications. In the first subsection I will display some results in the realm of the ultrarelativistic regime. In the second subsection I will present some preliminary general-relativistic stellar collapse calculations obtained with the general-relativistic version of our MUSCL-code.

8.1 Special-Relativistic Hydrodynamics: Ultrarelativistic Regime

The particularization of the relativistic hydrodynamic equations of the section §6 -system (49)- to the one-dimensional and planar case can be written

$$\frac{\partial \mathbf{u}}{\partial \mathrm{t}} + \frac{\partial \mathbf{f}(\mathbf{u})}{\partial \mathrm{x}} = 0 \tag{63}$$

being the 3-dimensional vector of unknowns $\mathbf{u}$

$$\mathbf{u} = (r, m, e)^{\mathrm{T}} \tag{64}$$

and the *flux* vector $\mathbf{f}(\mathbf{u})$

$$\mathbf{f} = \left(\frac{rm}{e+p}, \frac{m^2}{e+p} + p, m(1 - \frac{r}{e+p}) \right)^{\mathrm{T}} \tag{65}$$

where we have introduced the following variables:

$$r \equiv \rho W \tag{66}$$

$$m \equiv \rho h W^2 v \tag{67}$$

$$e \equiv \rho h W^2 - p \tag{68}$$

From the set of conserved variables $\aleph = \{r, m, e\}$ we need to recover the set of physical variables $\wp = \{\rho, v, \epsilon\}$ at each time step; next, the pressure will be evaluated from the EOS and the loop is closed. The algorithm for going through the $\aleph$ variables to the $\wp$ variables is merely an algebraic equation in p for which powerful methods can be applied. This is the only small price to pay for having a system written in such a way that we can use *ad hoc* methods. Writing the system in the above *conservation form* allowed us to efficiently use high-resolution methods in order to approximate its solutions.

The spectral decomposition of the Jacobian matrix associated to the flux can be found in references [44] or [19].

Our relativistic hydro-code has overcome several severe standard tests: *the relativistic Sod's test*, *the relativistic blast wave* and *the relativistic shock reflection*. Let me focus on the last one in this talk. Interested readers can be address to the references [44] and [41].

We have computed the solution to the *relativistic shock reflection* problem, that is, the shock thermalization of a cold, relativistically moving gas hitting a wall. Initial conditions are: $\rho = \rho_1 = 1$, $v = v_1$ and $\epsilon = 0$. An ideal gas law of adiabatic index $\Gamma = 5/3$ has been assumed.

The gas behind the shock is at rest ($v_2 = 0$) but its density increases with the initial velocity according to the following compression ratio σ ($\equiv \rho_2/\rho_1$)

$$\sigma = \frac{\Gamma + 1}{\Gamma - 1} + \frac{\Gamma}{\Gamma - 1}\epsilon_2 \tag{69}$$

where $\epsilon_2 = W_1 - 1$ and subscripts 1 and 2 stand for the states of the gas ahead and behind, respectively, of the shock. As it is well-known, in the Newtonian limit the compression ratio is independent of the initial velocity. In the ultrarelativistic regime the density of the gas behind the shock can grow without any limit ($\sigma \sim W_1$).

We run our code for several values of v_1 so as to cover all regimes, from the Newtonian to the ultrarelativistic one. An Eulerian grid of 100 points has been used.

Figures 1, 2 and 3 (taken from [41]) show the pressure of the gas at some instant when the shock is well formed, and for $v_1 = 0.9, 0.99, 0.999$.

For the sake of comparison we have displayed the analytical solution (continuous line). The mean relative error in our calculation of σ is 0.1%. This should be compared with the 5.6% reported by Centrella and Wilson in [10], for $v_1 = 0.9$

($W_1 = 2.29$) -the highest value of v_1 for which Centrella and Wilson have published results-. In [44] we have arrived, with our MUSCL version, at $W_1 \approx 23$. Indeed, as we noticed in [44], the resolution of the shock is poorer - and needs eight or nine points- at $W_1 >> 1$, that is, when the difference between the light velocity and the initial velocity verifies $1 - v_1 \approx O(\Delta x^p)$, where p stands for the global accuracy of the algorithm. With PHM we have obtained very sharp shock profiles -see the pressure profile in figure 4 (taken from [41])- even when $v_1 = 0.9999$, i.e., $W_1 \approx 70$. The results are better than the ones reported by other authors (see, e.g., [32] or [53]) and, as far as we know, give the best resolution for fixed grids.

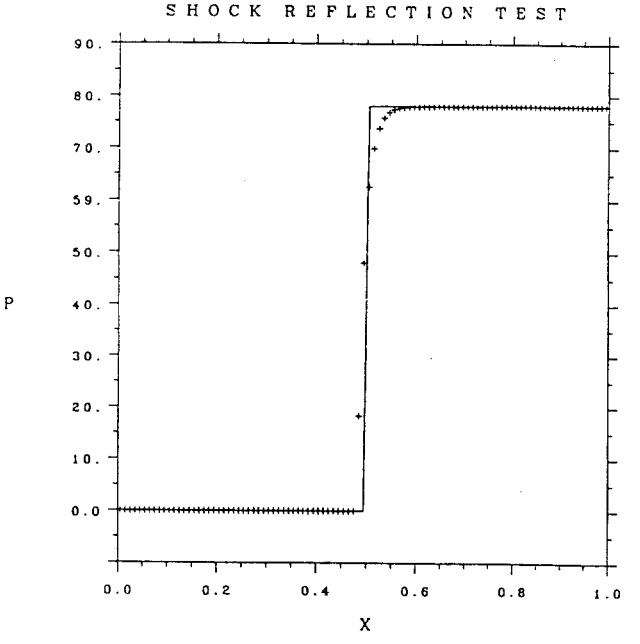

Fig. 2. Pressure in the *relativistic shock wall* test. Initial velocity is 0.99, in units of the speed of light

8.2 General-Relativistic Stellar Collapse

In a previous paper [42] Martí *et al.* focussed on the shock formation and propagation such as it appears in the standard scenario of the so-called *prompt mechanism* of type II Supernovae. In this reference [42] we have made a sample of Newtonian stellar collapse calculations with two codes: i) A standard finite-difference scheme which uses an artificial viscosity technique. ii) A Godunov-type method which uses a linearized Riemann solver. The initial model and the equation of state was kept fixed in order to be able to compare both methods directly. Differences in the behaviour of the global energetics of the collapse

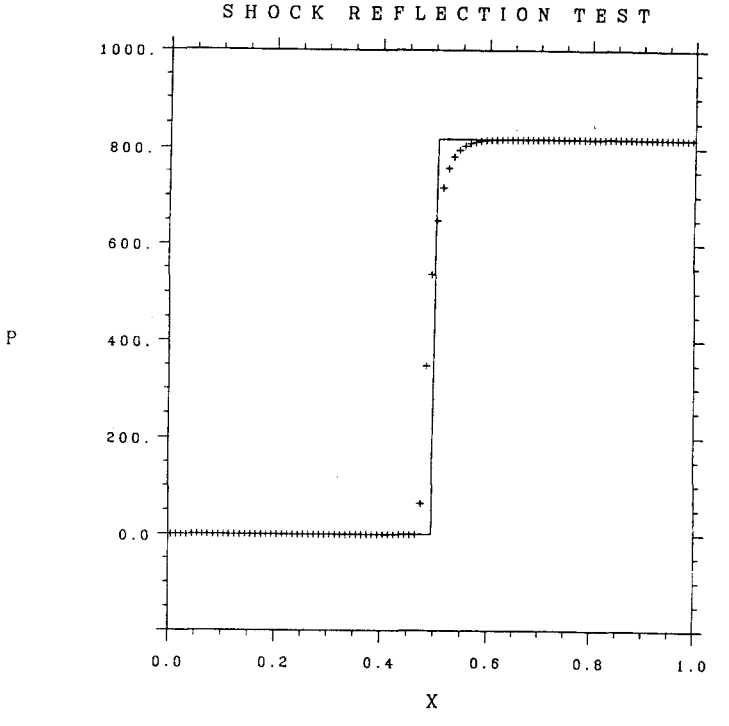

Fig. 3. Pressure in the *relativistic shock wall* test. Initial velocity is 0.999, in units of the speed of light

were found to depend on the particular way in which the artificial viscosity is implemented. Although the grid used was rather poor (only 50 nodes) and more sophisticated forms for the artificial viscosity can be found in the literature (see the paper of Noh in [52], referenced in section §3) our results in [42] might be of interest not only in the field of the *prompt mechanism* of Type II Supernovae, but even in the correct estimation of the efficiency of the energy released in form of gravitational radiation in non-spherical collapse. Indeed, as Bonazzola and Marck (in [4]) have emphasized, the gravitational power decreases with viscosity, ν, as $1/\nu^6$; hence, viscosity of a numerical code -explicit or intrinsic- may have dramatic effects.

The equations of general-relativistic hydrodynamics are the expression of the local laws of conservation of baryon number density and energy-momentum in a space-time $\mathcal{M}$, described by the four dimensional metric tensor $g_{\mu\nu}$. In our procedure, the metric is split into the objects α and γ_{ij}, keeping the line element in the form:

$$ds^2 = -\alpha^2 dt^2 + \gamma_{ij} dx^i dx^j \tag{70}$$

By defining the following set of variables

$$D \equiv \rho W$$

$$S \equiv \alpha T^{0r} = \rho h W^2 v$$

$$\tau \equiv \alpha^2 T^{00} = \rho h W^2 - p$$

the general-relativistic hydrodynamic equations in the one dimensional case (for example, spherical symmetry) can be written as a system of conservation laws in the sense of Lax [36]:

$$\frac{\partial \mathbf{u}}{\partial t} + \frac{\partial \mathbf{f(u)}}{\partial r} = \mathbf{s(u)}, \tag{71}$$

where

$$\mathbf{u} = (D, S, \tau)^{\mathrm{T}}$$

is the 3-dimensional vector of unknowns which defines the state of the system, the fluxes are

$$\mathbf{f} = \frac{\alpha}{\sqrt{\gamma_{rr}}} \left(\frac{DS}{\tau + p}, \frac{S^2}{\tau + p} + p, S \right)^T,$$

and the source terms are free of derivatives of hydrodynamic quantities and read:

$$\begin{aligned} \mathbf{s(u)} = \Bigg(& -D \frac{\partial ln\sqrt{\gamma}}{\partial t} - \frac{\alpha}{\sqrt{\gamma_{rr}}} \frac{DS}{\tau + p} \frac{\partial ln\gamma}{\partial r}, \\ & - S \frac{\partial ln(\sqrt{\gamma \gamma_{rr}})}{\partial t} - \frac{\alpha}{\sqrt{\gamma_{rr}}} \left[\left(\frac{S^2}{\tau + p} \right) \frac{\partial ln\sqrt{\gamma}}{\partial r} + \tau \frac{\partial ln\alpha}{\partial r} + p \frac{\partial ln\sqrt{\gamma_{rr}}}{\partial r} \right], \\ & - \tau \frac{\partial ln\sqrt{\gamma}}{\partial t} - \frac{\alpha}{\sqrt{\gamma_{rr}}} S \frac{\partial ln\alpha\sqrt{\gamma}}{\partial r} - \frac{S^2}{\tau + p} \frac{\partial ln\sqrt{\gamma_{rr}}}{\partial t} - p \frac{\partial ln\sqrt{\gamma}}{\partial t} \Bigg)^T \end{aligned}$$

In the above expressions, quantity γ is the determinant of the matrix γ_{ij}, v is defined by $v \equiv \sqrt{\gamma_{rr}} u^r / \alpha u^0$ (indexes 0 and r stands for the temporal and radial components, respectively) and represents the fluid velocity relative to an inertial observer at rest in the coordinate frame. The Lorentz-like factor is defined by $W \equiv \alpha u^0$.

From the *conserved* quantities $\aleph = \{D, S, \tau\}$, as in the special-relativistic case, we must obtain the set of quantities $\wp = \{\rho, v, \epsilon\}$ at each time step, by solving an implicit equation for pressure. In the Newtonian limit, the set of new variables $\aleph = \{D, S, \tau - D\}$ tends to the set $\{\rho, \rho v, \rho\epsilon + (1/2)\rho v^2\}$.

The hyperbolic character of the above system of equations as well as the spectral decomposition of the Jacobian matrix associated to the flux has been discussed in references [44], [43] and [34].

We have tested our one-dimensional general-relativistic code to reproduce some of the stationary solutions of the *spherical accretion onto a black hole* in two cases: i) *dust* accreting onto a Schwarzschild black hole [32] and ii) an *ideal gas* accreting onto a Schwarzschild black hole [45]. Details of these numerical experiments can be found in [43].

The initial model we have taken in our stellar collapse calculations is a white dwarf-like configuration having a central density $2.5 \times 10^{10}\ g/cm^3$. This is an equilibrium model for a particular EOS (Chandrasekhar's EOS with coulombian corrections) corresponding to the maximum of the "mass-radius" curve (see [33]). The numerical grid has been built up in such a way that the radius of the initial

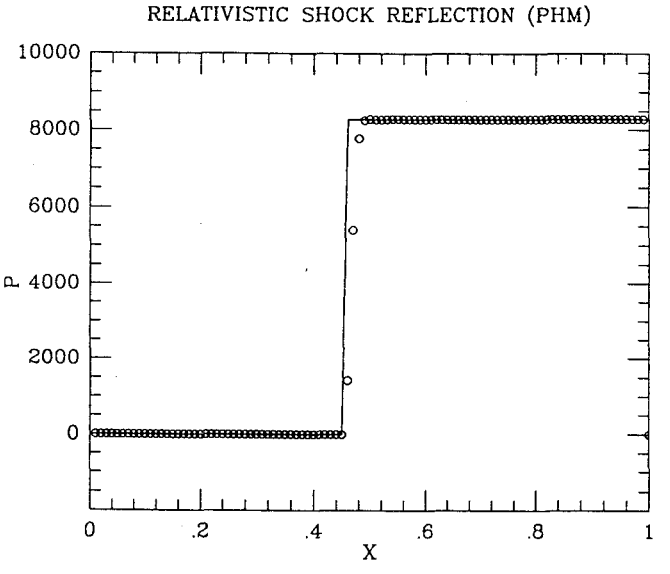

Fig. 4. Pressure in the *relativistic shock wall* test. Initial velocity is 0.9999, in units of the speed of light. PHM algorithm

model is partitioned into 200 zones distributed in geometric progression in order to have a finer resolution near the centre.

The EOS we have used is a Γ-law such that Γ varies with density according to Van Riper's prescription [66]:

$$\Gamma = \Gamma_{min} + \eta(\log\rho - \log\rho_b) \tag{72}$$

with: $\eta = 0$ if $\rho < \rho_b$ and $\eta > 0$ otherwise.

The parameters Γ_{min}, η and ρ_b are, typically: 4/3, 1, and $2.7\times\ 10^{14}$ gcm^{-3}, respectively, but we have also considered other values for Γ_{min} and η .

In these proceedings (see [3] in this volume) we present some results obtained using a harmonic time coordinate due to its singularity avoidance properties.

If we choose Schwarzschild-type coordinates (see, e.g., [8] or [26]) the full one-dimensional general-relativistic equations can be reduced to a merely hydrodynamical problem. In these coordinates the 3-metric reads

$$\gamma_{ij} = diag(X^2, r^2, r^2 sin^2\theta)$$

being

$$X = (1 - 2m/r)^{-1/2} \quad , \; m = m(r,t)$$

The source terms have been explicitly written in reference [34].

At each time step functions m and α are integrated along the radius according to

$$\frac{\partial m}{\partial r} = 4\pi r^2(\tau + D)$$

$$\frac{\partial ln\alpha}{\partial r} = X^2\left(\frac{m}{r^2} + 4\pi r(p + Sv)\right)$$

Let me notice the behaviour of the velocity field shown in figure 5 (taken from [34]). Shock is sharply solved in two zones and is free of spurious oscillations. The minimum of velocity -at the infall epoch- is about -0.40, that is $\approx 25\%$ greater than the value reported by [42], in the Newtonian case, for the same initial model, same EOS and a lagrangian version of our code which uses the same Riemann solver. The difference is entirely due to general-relativistic effects, although this point requires verification since a different grid has been used.

9 Multidimensional Problems

In two space dimensions a system of conservation laws takes the form

$$\frac{\partial \mathbf{u}}{\partial t} + \frac{\partial \mathbf{f(u)}}{\partial x} + \frac{\partial \mathbf{g(u)}}{\partial y} = 0 \tag{73}$$

where $\mathbf{u} = \mathbf{u}(x, y, t)$

The multidimensional character of the above system has been taken into account numerically by considering standard *operator splitting* techniques ([71]), similar to the ones used for treating the source terms, or the corresponding extension of the *method of lines* already discussed in section §7.

The splitting proceeds in two steps and the algorithm can be written -in a 2D case- as follows:

$$\mathbf{u}^{n+1} = \mathcal{L}_g^{\Delta t}\mathcal{L}_f^{\Delta t}\mathbf{u}^n \tag{74}$$

where $\mathcal{L}_f$ and $\mathcal{L}_g$ stand for the operators in finite differences associated, respectively, to the 1D systems

$$\frac{\partial \mathbf{u}}{\partial \mathrm{t}} + \frac{\partial \mathbf{f(u)}}{\partial \mathrm{x}} = 0$$

and

$$\frac{\partial \mathbf{u}}{\partial \mathrm{t}} + \frac{\partial \mathbf{g(u)}}{\partial \mathrm{y}} = 0$$

In this section I am going to discuss some multidimensional problems that we have used as bed-tests in our progress towards the construction of a multidimensional relativistic hydro-code. First, in subsection (§9.1) I will show the solution of some particular general-relativistic flows which can be described by a wave equation in a curved space-time. The next subsection (§9.2) is devoted to our preliminary results with relativistic multidimensional tests.

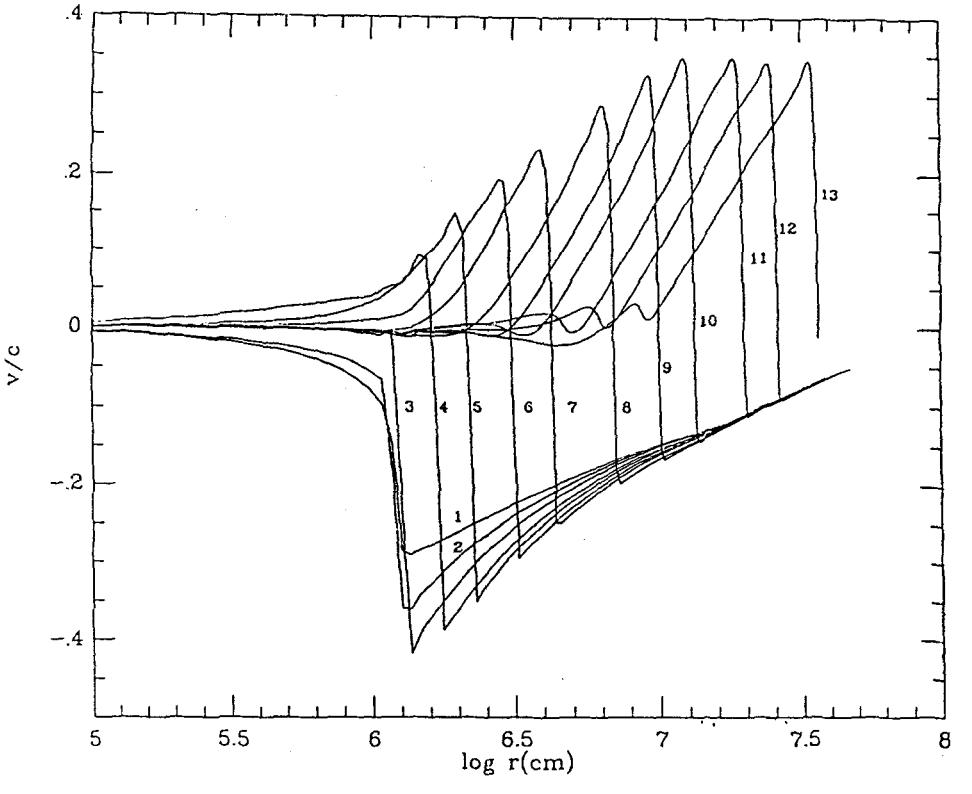

Fig. 5. General-relativistic stellar collapse. Snapshots of the velocity, in units of the speed of light, versus radial coordinate, in logarithmic scale and units of cm. Each curve is labeled by a number which establishes the temporal sequence into the interval $90.17 \leq t(msec.) \leq 93.34$

9.1 Potential flow passing over a black hole

In 1988 Petrich *et al.* (see [55]) derived, based on some assumptions, the analytical solution for the steady-state, subsonic accretion of a gas onto a Schwarzschild black hole. As a consequence of their assumptions the equations of general-relativistic hydrodynamics are simplified and lead to a wave equation for a potential ψ in a curved space-time:

$$\psi^{;\mu}_{,\mu} = 0 \tag{75}$$

where ; and , stand, respectively, for the usual covariant and ordinary derivatives.

From this potential ψ the velocity field can be derived:

$$hu_\mu = \frac{\partial \psi}{\partial x^\mu} \tag{76}$$

In the Schwarzschild gravitational field generated by a source of mass M this equation reads

$$\frac{1}{r^2}\frac{\partial}{\partial r}\left[\left(1-\frac{2M}{r}\right)r^2\frac{\partial\psi}{\partial r}\right]+\frac{1}{r^2}\left[\frac{1}{sin\theta}\frac{\partial}{\partial\theta}\left(sin\theta\frac{\partial\psi}{\partial\theta}\right)+\frac{1}{sin^2\theta}\frac{\partial^2\psi}{\partial\phi^2}\right]- \\ -\left(1-\frac{2M}{r}\right)^{-1}\frac{\partial^2\psi}{\partial t^2}=0 \tag{77}$$

A stationary solution of this equation which satisfies the appropriate boundary conditions (see [55]) is

$$\psi = -u^0_\infty t - 2Mu^0_\infty ln(1-2M/r) + u_\infty(r-M)cos\theta \tag{78}$$

for a black hole. Here u^0_∞ and u_∞ are the asymptotic values of the temporal component of the four-velocity and the modulus of the three-vector $\mathbf{u}$, respectively. Let us notice the following relations between u^μ_∞ and the three-velocity vector $\mathbf{v}_\infty$

$$u^\mu_\infty = (u^0_\infty, \mathbf{u}_\infty) = (1-v^2_\infty)^{-1/2}(1, \mathbf{v}_\infty) \tag{79}$$

where v_∞ is the absolute value of the asymptotic fluid three-velocity.

Although the above particular potential flow problem does not allow the presence of shock waves we have used this problem as a test of our 2D-MUSCL algorithm in order to describe the non-linearities induced by the geometrical terms related with the strong gravitational fields. With this aim, the above wave equation (77) has been rewritten as a hyperbolic system of conservation laws -in the sense of Lax [36]- by splitting it into a system of three equations of first order.

To do this let us introduce the following auxiliary functions

$$a = \frac{\partial\psi}{\partial t} \quad b = \frac{\partial\psi}{\partial r} \quad c = \frac{\partial\psi}{\partial\theta} \tag{80}$$

The hyperbolic system of conservation laws equivalent to (77) is

$$\frac{\partial \mathbf{u}}{\partial t} + \frac{\partial \mathbf{f(u)}}{\partial r} + \frac{\partial \mathbf{g(u)}}{\partial \theta} = \mathbf{s(u)} \tag{81}$$

where

$$\mathbf{u} = (a, b, c) \tag{82}$$

is the 3-dimensional vector of unknowns, and

$$\mathbf{f}(\mathbf{u}) = \left(-(1-\frac{2M}{r})^2 b, -a, 0\right) \tag{83}$$

and

$$\mathbf{g}(\mathbf{u}) = \left(-(1-\frac{2M}{r})\frac{1}{r^2}c, 0, -a\right) \tag{84}$$

are the 3-vector-valued functions defining the *fluxes* in the r and θ directions, respectively. Finally

$$\mathbf{s}(\mathbf{u}) = \left((1-\frac{2M}{r})(1-\frac{3M}{r})\frac{2}{r}b + (1-\frac{2M}{r})\frac{\cos\theta}{r^2\sin\theta}c, 0, 0\right)$$

are the *source* terms.

In this application the source terms have been treated by operator splitting techniques in such a way that the operator associated to the source sector is the one which solves the system

$$\frac{\partial \mathbf{u}}{\partial \mathrm{t}} = \mathbf{s}(\mathbf{u})$$

in the following form

$$[\mathbf{I} - \frac{1}{4}\Delta t \mathbf{s}'(\mathbf{u}_i^n)]\Delta \mathbf{u}_i^* = \frac{1}{2}\Delta t \mathbf{s}(\mathbf{u}_i^n)$$
$$\mathbf{u}_i^* = \mathbf{u}_i^n + \Delta \mathbf{u}_i^*$$

where $\mathbf{s}' = \frac{\partial \mathbf{s}}{\partial \mathbf{u}}$.

The spectral decomposition of the Jacobian matrices associated to the fluxes in each direction as well as the characteristics of the computational cell and the initial and boundary conditions of our application can be found in reference [17].

In figure 6 (taken from [17]) we can see the evolution towards the steady-state accretion reached in a time $t \approx 65M$ for an asymptotic velocity $v_\infty^2 = 0.7$. This sequence of figures shows the flow lines for the following values of the temporal coordinate (in units of M): 0, 3.5, 65 and 100. We have obtained a value of $3.42 \leq r_A/M \leq 3.95$ (this interval is constrained by the resolution of our grid) for the radius of the critical cylinder inside which material is ultimately captured by the black hole, being the exact value $3.404M$ for an asymptotic velocity $v_\infty^2 = 0.7$.

The main conclusion from these figures is the following: we have succeeded in obtaining the stationary solution by using a *modern high-resolution shock-capturing* scheme of second order.

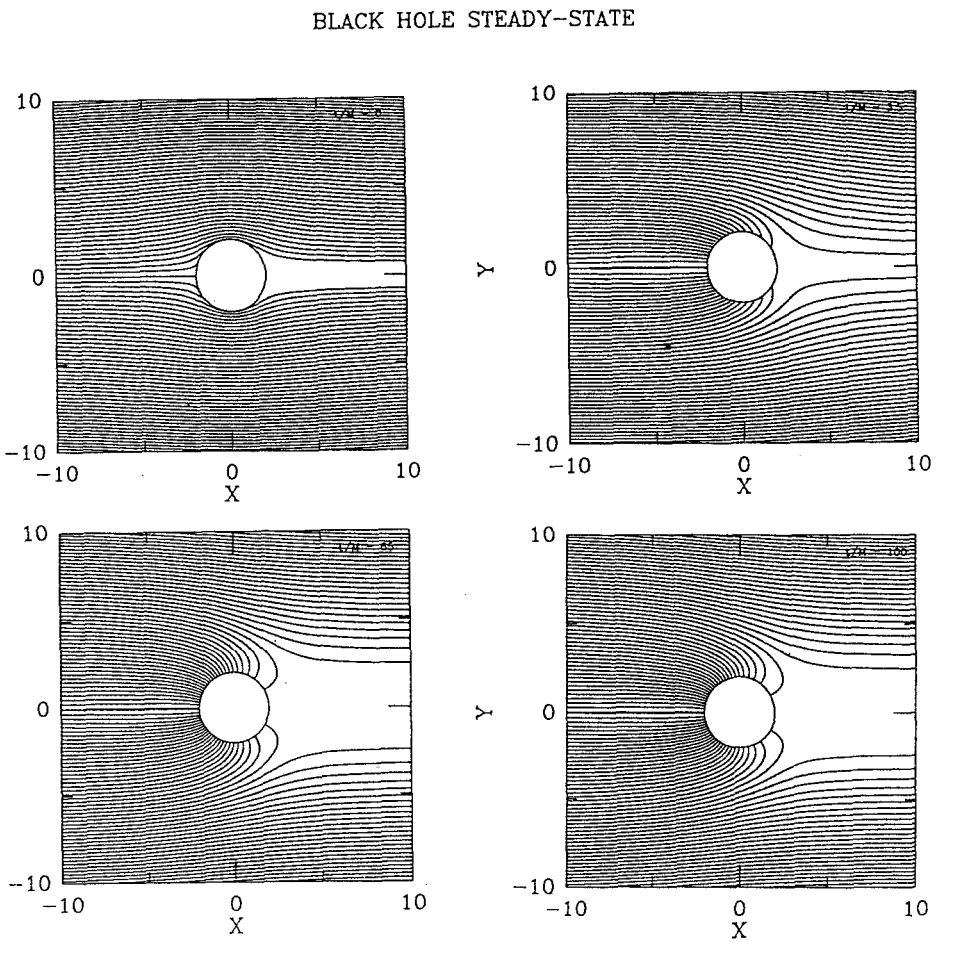

Fig. 6. Potential flow passing over a black hole. Evolution towards the steady-state accretion reached in a time $t \approx 65M$ for an asymptotic velocity $v_\infty^2 = 0.7$

9.2 2D Relativistic Hydrodynamics

As a first step to our objective of designing a multidimensional hydro-code to deal with the equations of relativistic hydrodynamics we built up a Newtonian two-dimensional hydro-code which has overcome the standard and severe test due to Emery (see below). Details concerning our Newtonian hydro-code can be found in [18].

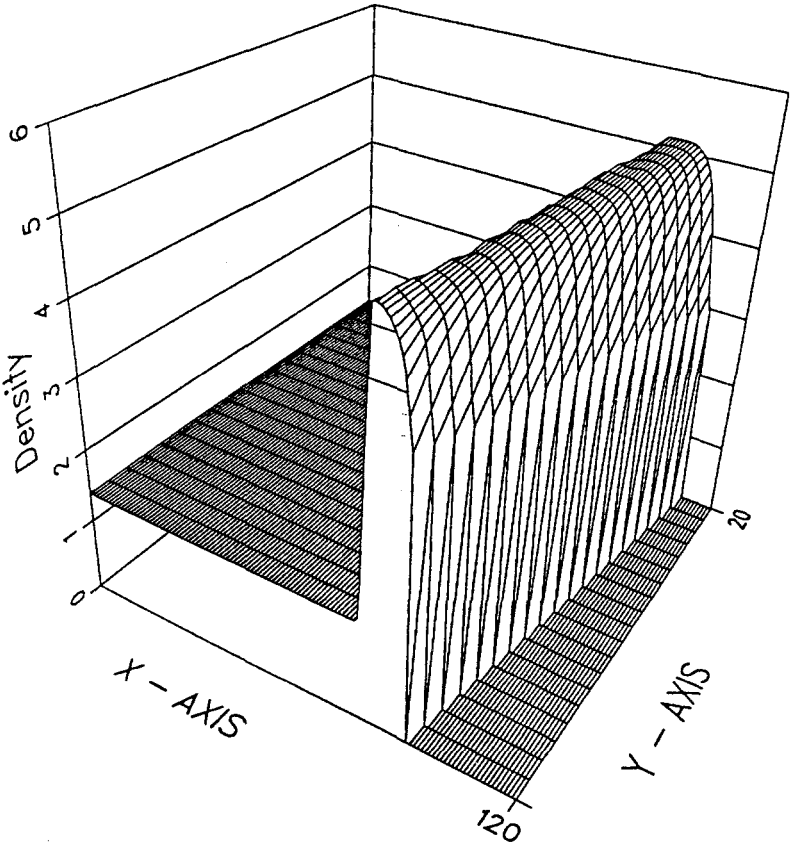

Fig. 7. Steady relativistic oblique shock. Initial inflow velocity 0.01 (in units of the speed of light). See text for details

Joining together the algebraic relations discussed in section §6 and the basic ingredients of our 2D MUSCL algorithm, once it has been tested with the above Newtonian numerical experiment, we are ready to show our preliminary

relativistic results. These are -as far as we know- the first ones (in scientific literature) which have made use of modern high-resolution shock-capturing techniques in the realm of multidimensional relativistic hydrodynamics. Their interest goes further away of the special-relativistic case if we keep into account that, as it is well-known and we have shown in our 1D general-relativistic applications, the equivalence principle warranties the feasibility of extending our procedure to the study of test fluids evolving in strong gravitational fields.

The equations describing the two-dimensional flow of a relativistic ideal fluid are the trivial particularization of the ones displayed in section §6. The spectral decomposition of the Jacobian matrices associated to the fluxes in each direction have been derived in reference [19].

Let me display two numerical tests we have carried out with our relativistic 2D MUSCL code: i) the steady *relativistic oblique shock* wave, and ii) the relativistic version of the *Emery's step.*

Relativistic Oblique shock The basic algebraic relations which connect the two states at each side of a steady relativistic oblique shock have been derived by Königl (see reference [35]) for ideal gases with a constant adiabatic index Γ. A fundamental difference between the Newtonian and relativistic descriptions is the fact that the jump in density increases, in the relativistic case, with the upstream velocity and tends to infinity in the extreme-relativistic regime. Königl derives an algebraic equation which defines implicitly the jump in velocities in terms of the known upstream state. Once the jump in velocities is calculated the remaining unknowns are easily obtained (see [35], for details).

We have generated an oblique shock throwing an ideal gas with $\Gamma = 7/5$ through a corner (an oblique plane) with a wedge angle of 28°. The initial density is 1.4 and the pressure the one resulting for a Mach 3 flow (Newtonian definition). The initial velocity (in units of the speed of light) runs, in our experiments, from 0.01 to 0.95. Figures 7 and 8 (taken from [19]) show the density as a function of the spatial coordinates and at some instant in its evolution when the steady state has been reached.

The solution looks like the Newtonian. This can be explained if we take into account that as several authors have emphasized (see, e.g., [70] or [35]) the equations of steady special-relativistic gas dynamics and steady non-relativistic gas dynamics have a similar mathematical form, when expressed in some appropriate variables. This property has been used in order to find numerical solutions for relativistic steady flows.

As we can see in figures 7 and 8, the qualitative behaviour of density is the one described above, being the particular numbers agree with the Königl relations.

Relativistic Emery's step A severe test for two-dimensional flows in presence of shocks is the flat-faced step originally introduced by Emery (1968): a Mach 3 flow is injected into a tunnel containing a step. The tunnel is 3 units long and 1 unit wide. The step is 0.2 units high and is located 0.6 units from the left-hand end of the tunnel. Slab symmetry is assumed.

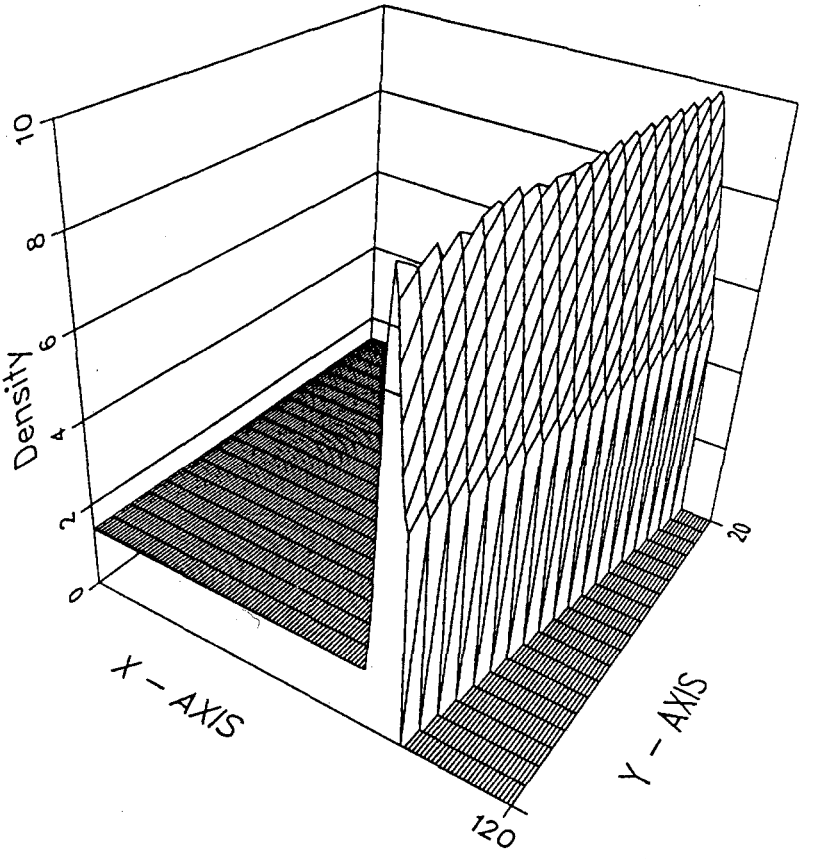

Fig. 8. Steady relativistic oblique shock. Initial inflow velocity 0.95 (in units of the speed of light). See text for details

The boundary conditions are: 1) Reflecting boundary conditions along the walls of the tunnel and at the left face and the bottom of the step. 2) On the right and the left sides of the tunnel, respectively, outflow and inflow boundary conditions are applied.

The initial conditions for the gas in the tunnel are given by

$$\rho(x, y, 0) = \rho_0 = 1.4$$

$$v^x(x, y, 0) = v_0^x$$

$$v^y(x, y, 0) = v_0^y = 0$$

for all x, y. The value of the initial pressure is derived from the other variables. The initial value of the x-component of the three-velocity v_0^x will be a free parameter.

The EOS considered is the one of an ideal gas with $\Gamma = 7/5$. Gas is continually fed in at the left-hand boundary with the flow variables given by their initial values. A rectangular grid of 120×40 has been used.

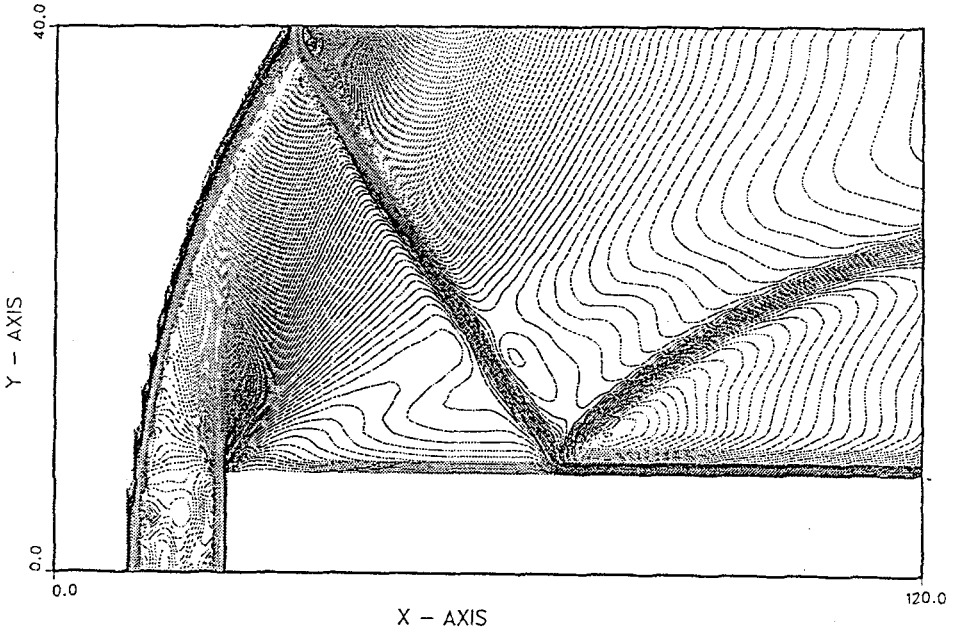

Fig. 9. Relativistic Emery's step. See text for details

As we have mentioned at the beginning of this section, an operator splitting technique in each spatial direction has been performed. We have also experimented with methods which avoid the splitting in spatial directions and which

permit advancing in time with the third order Runge-Kutta method previously explained. In this last line of experimentation we have observed an important reduction of numerical noise and the best results have been obtained.

At the transonic rarefactions, where entropy violation may appear (and, in fact, it does), a local artificial viscosity according to the prescription of Harten and Hymann (1983) was incorporated.

Figure 9 (taken from [19]) shows the isodensity curves of the system at some instant of its evolution ($v_0^x = 0.9$). The main features of the solution are the Mach reflection of a *bow shock* at the upper wall, making the density distribution the most difficult to compute, and a *rarefaction fan* centered at the corner of the step. These general characteristics of the solution are similar to those found in the Newtonian case. Currently, we are experimenting with higher inflow velocities.

The severity of this test makes us confident of the feasibility of astrophysical applications as complex as the ones mentioned in the introduction of this paper.

10 Conclusions

1. We have extended some *high-resolution shock-capturing methods* (avoiding the use of an artificial viscosity in treating strong discontinuities) to the relativistic hydrodynamic system of equations.
   - The equations of relativistic hydrodynamics have been written in terms of a well-defined set of variables for which the system exhibits their conservative character.
   - We have compared two *high-resolution shock-capturing methods* : our version of MUSCL and PHM. Several standard and severe tests involving strong shocks have been successfully overcome. With PHM we have been able to reach Lorentz factors as high as $W \approx 70$ in the *relativistic normal reflection shock* problem.
2. We have computed the general-relativistic collapse of spherically symmetric configurations paying particular attention on the bounce and shock propagation.
3. We have succeeded in obtaining stationary solutions of general-relativistic potential flows in a Schwarzschild background.
4. By combining operator splitting techniques with the corresponding theoretical analysis of the spectral decomposition of the Jacobian matrices associated with each direction of the fluxes we have explored the realm of multidimensional relativistic hydrodynamics.
   - With our MUSCL code we have solved the relativistic oblique shock. In these experiments, the initial velocity of the supersonic flow (Mach 3) spans the interval $0.01 \leq v_1 \leq 0.95$ Our results accord with the analytical ones.
   - The severe Emery's step test has been overcome in its relativistic version.

The above conclusions give us confidence in the feasibility of our procedure to extend modern high-resolution shock-capturing methods to the multidimensional relativistic hydrodynamics. Some of the results shown in this lecture -in particular, those indicated in items 2 and 4- are, as far as we know, entirely new.

Acknowledgments

This work has been supported by the Spanish DGICYT (reference numbers PB90-0516-C02-02 and PB91-0648).

References

1. A.M. Anile, *Relativistic fluids and magneto-fluids*, Cambridge University Press (1989).
2. M.C. Begelman, R.D. Blandford, and M.J. Rees, Rev. Mod. Phys., **56**, 255 (1984).
3. C. Bona, J.M^{a}. Ibáñez, J.M^{a}. Martí and J. Massó, *Shock-capturing methods in 1D Numerical Relativity*, this volume (1992).
4. S. Bonazzola and J.A. Marck, in *Frontiers in Numerical Relativity*, ed. by Evans C.R. and Finn L.S., p. 239, Cambridge University Press (1989).
5. S. Bonazzola and J.A. Marck, J. Comp. Phys., **87**, 201 (1990).
6. S. Bonazzola and J.A. Marck, J. Comp. Phys., **97**, 535 (1991).
7. S. Bonazzola and J.A. Marck, in *Approaches on Numerical Relativity*, ed. by D'Inverno, Cambridge University Press (1992), *in press.*
8. H. Bondi, Proc. Royal Soc. of London, **A281**, 39 (1964).
9. G.E. Brown, H.A. Bethe, and G. Baym, Nucl. Phys., **A375**, 481 (1982).
10. J. Centrella, and J.R. Wilson, Ap. J. Suppl., **54**, 229 (1984).
11. P. Colella, and P.R. Woodward, J. Comp. Phys., **54**, 174 (1984).
12. P. Colella, and H.M. Glaz, J. Comp. Phys., **59**, 264 (1985);
13. R. Courant, E. Isaacson, and M. Rees, Comm. Pure Appl. Math., **5**, 243 (1952).
14. B. Einfeldt, SIAM J. Num. Anal., **25**, 294 (1988).
15. A.F. Emery, J. Comp. Phys., **2**, 306 (1968).
16. C. R. Evans, in *Dynamical space-times and numerical relativity* , ed. by J. Centrella (Cambridge University Press, 1986).
17. J.A. Font, J.M^{a}. Martí, J.M^{a}. Ibáñez and J.A. Miralles, Comput. Phys. Comm., submitted (1992).
18. J.A. Font, J.M^{a}. Ibáñez and J.M^{a}. Martí, *in preparation* (1992).
19. J.A. Font, J.M^{a}. Ibáñez A. Marquina and J.M^{a}. Martí, *in preparation* (1992).
20. H. Freistühler and E.B. Pitman, J. Comp. Phys., **100**, 306 (1992).
21. B.A. Fryxell, E. Müller, and W.D. Arnett, in *Numerical Methods in Astrophysics*, ed. P.R. Woodward (Academic Press) (1990).
22. R.A. Gingold and J.J. Monaghan, Mon.Not.R.Astron.Soc., **181**, 375 (1977).
23. P. Glaister, J. Comp. Phys., **74**, 382 (1988).
24. S.K. Godunov, Matematicheskii Sbornik, **47**, 271 (1959).
25. D. Gottlieb and S. Orszag, *Numerical Analysis of Spectral Methods.: Theory and Application*, Regional Conference Series Lectures in Applied Mathematics, **26** (SIAM, Philadelphia,1977).
26. E. Gourgoulhon, Astron. and Astrophys., **252**, 651 (1992).
27. A. Harten, B. Engquist, S. Osher, S. Chakravarthy, J. Comp. Phys., **71**, 231 (1987).

28. A. Harten, J.M. Hyman, and P.D. Lax, Comm. Pure Appl. Math., **29**, 297 (1976).
29. A. Harten and J.M. Hyman, J. Comp. Phys., **50**, 235 (1983).
30. A. Harten, P.D. Lax and B. Van Leer, SIAM Rev., **25**, 35 (1983).
31. A. Harten, and S. Osher, SIAM J. Num. Anal., **24**, 279 (1987).
32. J.F. Hawley, L.L. Smarr, and J.R. Wilson, Ap. J. Suppl., **55**, 211 (1984).
33. J.M^{a}. Ibáñez, Astron. and Astrophys., **135**, 382 (1984).
34. J.M^{a}. Ibáñez, J.M^{a}. Martí, J.A. Miralles and V. Romero, in *Approaches on Numerical Relativity*, ed. by D'Inverno, Cambridge University Press (1992), *in press.*
35. A. Königl, Phys. Fluids, **23**, 1083 (1980).
36. P.D. Lax *Regional Conference ,Series Lectures in Applied Math.*, **11** (SIAM, Philadelphia,1973).
37. P.D. Lax, and B. Wendroff, Comm. Pure Appl. Math., **13**, 217 (1960).
38. L.B. Lucy, Astron. J.,**82**, 1013 (1977).
39. P.J. Mann, Comput. Phys. Comm., **67**, 245 (1991).
40. A. Marquina, SIAM J. Scient. Stat. Comp., *in press* (1992).
41. A. Marquina, J.M^{a}. Martí, J.M^{a}. Ibáñez, J.A. Miralles and R. Donat, Astron. and Astrophys., **258**, 566 (1992).
42. J.M^{a}. Martí, J.M^{a}. Ibáñez, and J.A. Miralles, Astron. and Astrophys., **235**, 535 (1990).
43. J.M^{a}. Martí, *Ph.D. Thesis*, University of Valencia (1991).
44. J.M^{a}. Martí, J.M^{a}. Ibáñez and J.A. Miralles, Phys. Rev., **D43**, 3794 (1991).
45. F.C. Michel, Ap. Space Sci., **15**, 153 (1972).
46. J.C. Miller and O. Pantano, Phys. Rev., **D40**, 1789 (1989).
47. J.J. Monaghan and R.A. Gingold, J. Comp. Phys., **52**, 374 (1983).
48. J.J. Monaghan, Ann. Rev. Astron. Astrophys., **30**, 543 (1992).
49. T. Nakamura, Prog. Teor. Phys., **65**, 1876 (1981).
50. T. Nakamura, K. Maeda, S. Miyama and M. Sasaki, Prog. Teor. Phys., **63**, 1229 (1980).
51. T. Nakamura and H. Sato, Prog. Teor. Phys., **67**, 1396 (1982).
52. W.F. Noh, J. Comp. Phys., **72**, 78 (1987).
53. M.L. Norman, and K-H.A. Winkler, in *Astrophysical Radiation Hydrodynamics*, ed. by M.L. Norman, and K-H.A. Winkler (Reidel, 1986).
54. O.A. Oleinik, Usp. Mat. Nauk., **12**, 3 (1957); Engl. transl., Am. Mat. Soc. Transl. Ser. 2, **26**, 95 (1963).
55. L.I.Petrich, S.L. Shapiro and S.A.Teukolsky, Phys. Rev. Lett., **60**, 1781 (1988).
56. T. Piran, J. Comp. Phys., **35**, 254 (1980).
57. R. Richtmyer and K. Morton, *Difference Methods for Initial-Value Problems*, 2nd. ed., (Interscience, 1967).
58. P.L. Roe, J. Comp. Phys., **43**, 357 (1981).
59. S.L. Shapiro and S.A. Teukolsky, in *Black Holes, White Dwarfs and Neutron Stars* (Wiley, 1983).
60. C.W. Shu and S.J. Osher, J. Comp. Phys., **83**, 32 (1989).
61. R. F. Stark and T. Piran, Comp. Phys. Rept., **5**, 221 (1987).
62. M. Steinmetz and E. Müller, preprint from Max-Planck-Institut für Astrophysik, *submitted to Astron. and Astrophys.* (1992).
63. B. Van Leer, J. Comp. Phys., **23**, 276 (1977).
64. B. Van Leer, J. Comp. Phys., **32**, 101 (1979).
65. B. Van Leer, SIAM J. Sci. Stat. Comput., **5**,1 (1984).
66. K.A. Van Riper, Ap. J., **221**, 304 (1978).

67. J. Von Neumann, and R. Richtmyer, J. of Appl. Phys., **21**, 232 (1950).
68. J.R. Wilson, Astrophys. J., **173**, 431 (1972).
69. J.R. Wilson, in *Sources of gravitational radiation* , ed. L.L. Smarr (Cambridge University Press, 1979).
70. M.J. Wilson, Mon. Not. R. Astr. Soc., **226**, 447 (1987).
71. H.C. Yee, *VKI Lecture Notes in Computational Fluid Dynamics*, von Karman Institute for Fluid Dynamics, Belgium (1989).